RSC Advances

ROYAL SOCIETY OF CHEMISTRY

www.rsc.org/advances

High-performance hydrogen evolution electrocatalysis by layer-controlled MoS_2 nanosheets

Jiao Deng,[1] Wentao Yuan,[2] Pengju Ren,[1] Yong Wang,[2] Dehui Deng, [1]* Ze Zhang,[2] Xinhe Bao[1]

[1]State Key Laboratory of Catalysis, Dalian Institute of Chemical Physics, Chinese Academy of Sciences, Zhongshan Road 457, Dalian, 116023, China.

[2]Department of Materials Science and Engineering, Zhejiang University, Zheda Road 38, Hangzhou, ZheJiang, 310027, China.

*E-mail: dhdeng@dicp.ac.cn; Fax: +86-411-8469 4447; Tel: +86-411-8246 3003.

Abstract

Hydrogen is considered as an important clean energy carrier for the energy future and electrocatalytic splitting of water is one of the most efficient technologies for hydrogen production. As one potential alternative to Pt-based catalysts in hydrogen evolution reaction (HER), two-dimensional (2D) molybdenum sulfide (MoS_2) nanomaterials have evoked enormous research interest while it remains a great challenge in the structure control for high-performance HER electrocatalysis due to the lack of efficient preparation techniques. Herein, we reported a one-pot chemical method to directly synthesize 2D MoS_2 with controllable layers. Multiply-layer MoS_2 (ML-MoS_2), few-layer MoS_2 (FL-MoS_2) and single-layer MoS_2 coating on carbon nanotubes (SL-MoS_2-CNTs) can be efficiently prepared through the modulation of experimental conditions. The enhanced catalytic activity is demonstrated in HER with the layer number of MoS_2 nanosheets reducing. Remarkably, the optimized SL-MoS_2-CNTs sample showed long-term durability with an accelerated degradation experiment even more than 10,000 recycles, and high HER activity with an onset overpotential of only ~40 mV vs. RHE. This study introduces a novel, cheap and facile strategy to prepare layer-controlled 2D MoS_2 nanosheets with a large quantity, and are expected to broaden the already widely energy applications for 2D MoS_2 nanosheets.

Context

Two-dimensional (2D) molybdenum sulfide (MoS_2) nanomaterials have attracted great research interest because of its intriguing structural and electronic properties as well as the innumerous potential application in many energy fields, such as electronic devices,[1-3] lithium batteries[4-6] and electrocatalytic hydrogen evolution from water[7-10] etc. A bulk MoS_2 consists of many single-layer MoS_2 nanosheets, which are linked up by Van der Waals force, and each sheet is made up of a hexagonal layer of molybdenum atoms between two hexagonal layers of sulfur atoms. Previous studies indicate that few-layer, especially single-layer MoS_2 possesses distinctively different physical and chemical properties compared with their bulk materials, e.g. stronger photoluminescence,[11] greater luminescence quantum efficiency[12] and higher on-off ratio of transistors.[2, 13] Therefore, extensive efforts have been devoted to the preparation of few-layer and single-layer MoS_2 nanosheets. Presently, there are mainly two strategies, i.e. top-down methods including mechanical exfoliation,[14, 15] chemical exfoliation,[16, 17] electrochemical lithium intercalation,[18, 19] laser thinning[20] and ball milling,[21] and bottom-up methods including chemical vapor deposition on substrates[22, 23] and chemical synthesis.[18, 24, 25] Although significant progress has been made by many research groups, great challenge remains at the layer number control of these materials. Especially for the chemical synthesis methods in liquid phase, reaction intermediates are usually unstable and tend to form quasi-0D nanoparticles or 3D bulk materials during the preparation process.[26, 27]

Herein, we report a facile and scalable strategy for production of MoS_2 nanosheets with controllable layers via a direct chemical reaction of hexaammonium heptamolybdate ($(NH_4)_6Mo_7O_{24}$) and carbon disulfide (CS_2) under mild conditions. The layer number of MoS_2 nanosheets can be efficiently controlled through modulating the experimental conditions, i.e. synthesis process under H_2O-free environmental for multiply-layer MoS_2 (ML-MoS_2), and synthesis process within H_2O-assisted environmental for few-layer MoS_2 (FL-MoS_2). On the basis of this method, we can further prepare single-layer (SL) MoS_2 coating on carbon nanotubes (SL-MoS_2-CNTs) via adding CNTs in the precursors. This method can easily scale up

since the throughput is only limited by the size of the autoclave (more details see the experimental section in supporting information). The significantly enhanced catalytic activity is demonstrated in a hydrogen evolution reaction (HER) with the layer number of MoS_2 nanosheets reducing. Remarkably, the optimized SL-MoS_2-CNTs samples showed a long-term durability and high HER activity with an onset overpotential of only ~40 mV vs. RHE.

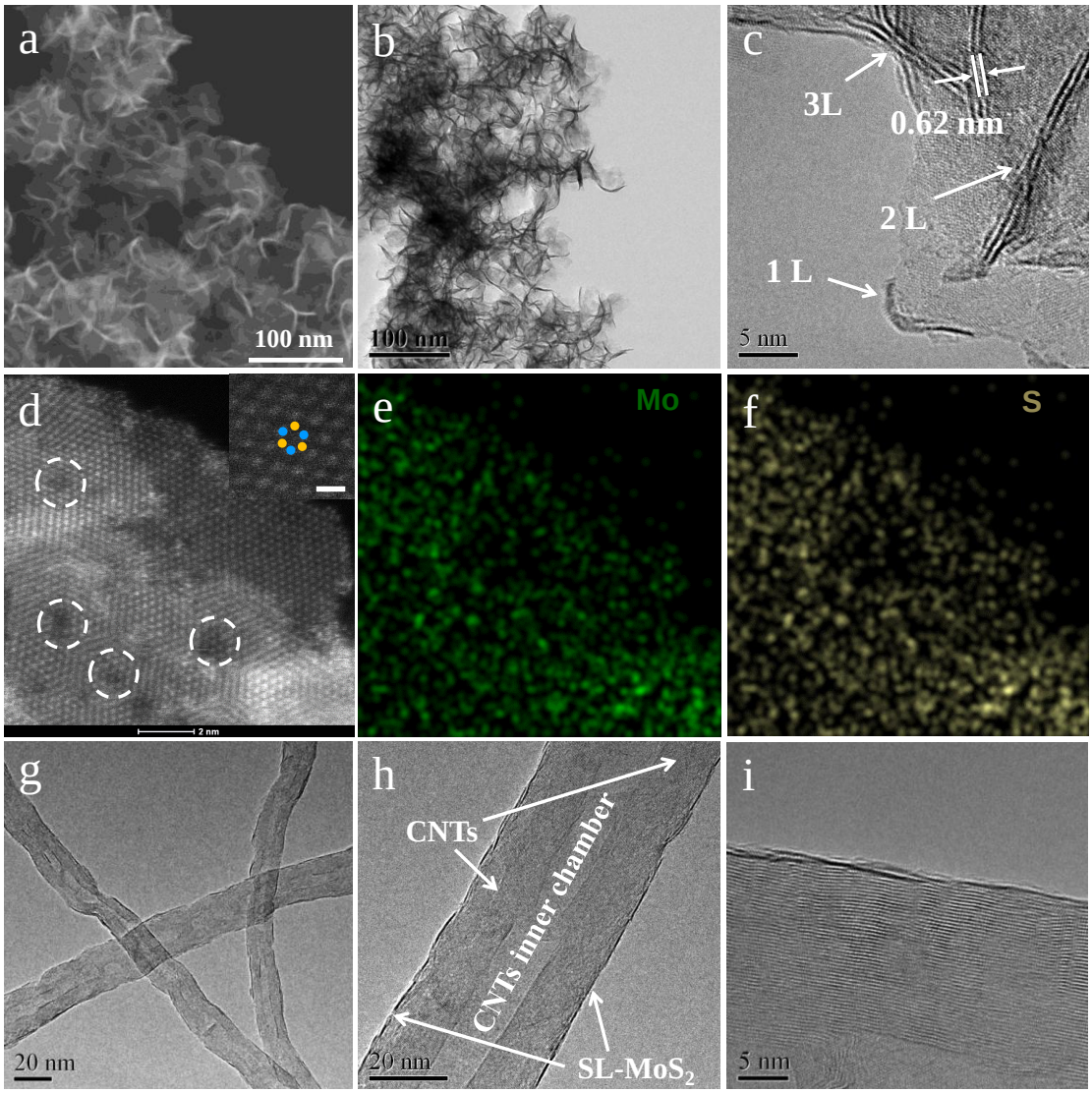

Figure 1. (a) SEM image of FL-MoS_2. (b) TEM image of FL-MoS_2. (c) HRTEM image of FL-MoS_2 with inset showing a layer distance of 0.62 nm. (d) HAADF-STEM image of FL-MoS_2 with the inset showing a honeycomb arrangement of MoS_2, blue and yellow dots in which represent Mo and S, respectively. The scale bar in the inset is 0.5 nm. The area with the dashed circles showing the defects in the

nanosheets. (e, f) EDX mapping images of Mo and S for FL-MoS_2 corresponding to figure (d). (g-i) HRTEM images of SL-MoS_2-CNTs.

The morphology and structure of MoS_2 nanosheets were examined by scanning electron microscopy (SEM) image and transmission electron microscopy (TEM) image. One can see that FL-MoS_2 exhibit a typical 3D flower-like morphology, which consists of the MoS_2 nanosheets (Figure 1a, b). Further high resolution (HR) TEM image shows that these nanosheets mainly contain 1-5 layers (L) (Figure S1d) with a layer distance of 0.62 nm, corresponding to the (002) plane of MoS_2 (Figure 1c). The sub-angstrom resolution high angle annular dark field-scanning transmission electron microscopy (HAADF-STEM) images (figure 1d, S2a) exhibit that honeycomb arrangement of the atoms extends over the entire nanosheets of FL-MoS_2, and the corresponding energy dispersive X-ray (EDX) mapping images reveal that the distribution of molybdenum atoms and sulfur atoms in the whole nanosheets is very homogeneous (figure 1e, 1f, S2b and S2c), further confirming the structural feature of MoS_2 nanosheets. In comparison, the ML-MoS_2 presents an irregular aggregation (Figure S3a) with an obvious thicker nanosheet structure compared with FL-MoS_2, i.e. the average layer number is c.a. 6 L for ML-MoS_2 and c.a. 3 L for FL-MoS_2, as the statistical analysis from the HRTEM images in figure 2b, S1d and S3d. In addition, when adding CNTs during the synthesis process, it is interesting to find that MoS_2 nanosheets trends to coat on CNTs continuously (figure 1g-i), and most of the layer number (more than 70%) is 1 L (figure 2b and S4d).

X-ray diffraction (XRD) and Raman spectroscopy were used to further analyze the layer structure of these MoS_2 samples. As XRD patterns in Figure 2a, all the samples exhibited the typical (002), (100), (103) and (110) planes of hexagonal 2H-MoS_2. Since (002) reflection of MoS_2 is the characteristic peak for the *c* axis and (100) for *ab* plane, we can take the intensity ratio between (002) and (100) peaks ($I_{(002)/(100)}$) of MoS_2 to assess the layer number variation in the series of these samples. One can see the ratio $I_{(002)/(100)}$ of bulk MoS_2 (22.67), ML-MoS_2 (1.69), FL-MoS_2 (0.85) and SL-MoS_2-CNTs (0.28) decreased gradually (figure 2b), indicating that the

layer number of these MoS_2 samples decreases in turn. In addition, all Raman spectrum (Figure 2c) of these MoS_2 samples showed the two characteristic peaks at 390 and 415 cm^{-1} corresponding to the E^1_{2g} and A_{1g} modes of hexagonal MoS_2 crystal, respectively. It is reported that the frequency of A_{1g} mode will have a red-shift with the layer number of MoS_2 decreasing.[28-30] As expected, an obvious red-shift of A_{1g} modes was observed from bulk MoS_2 to FL-MoS_2, indicating the layer number decreases gradually in these samples, in good agreement with the XRD and HRTEM analysis. Note that there was a slight blue-shift of A_{1g} modes from FL-MoS_2 to SL-MoS_2-CNTs, which was probably due to the presence of strain introduced by the curvature increase of MoS_2 nanosheets when coating onto the CNTs.[31, 32]

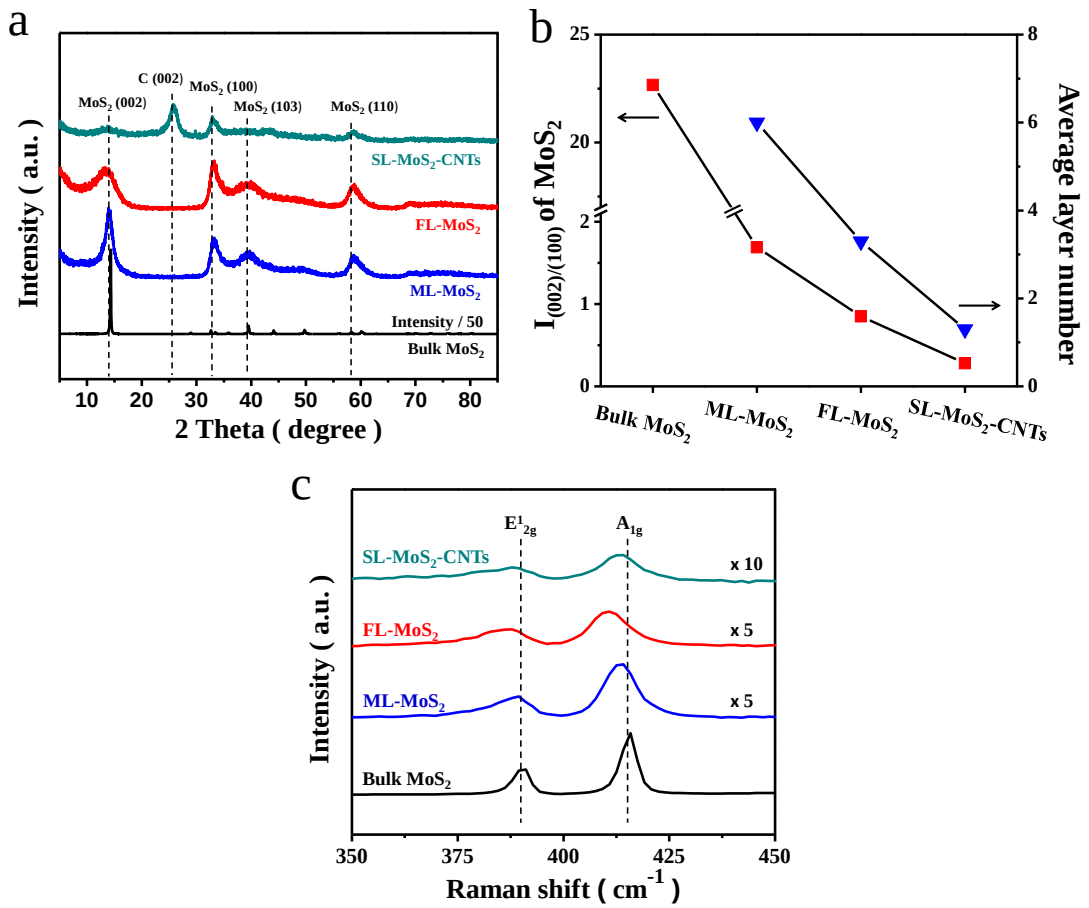

Figure 2. (a) XRD patterns of SL-MoS_2-CNTs, FL-MoS_2 and ML-MoS_2 in comparison to bulk MoS_2. (b) Intensity ratio of the MoS_2 (002) peak and MoS_2 (110) peak ($I_{(002)/(100)}$) for bulk MoS_2, ML-MoS_2, FL-MoS_2 and SL-MoS_2-CNTs in XRD, and the average layer number of ML-MoS_2, FL-MoS_2 and SL-MoS_2-CNTs obtained

from the statistical analysis by HRTEM in Figure S1, S3 and S4. (c) Raman spectra of SL-MoS_2-CNTs, FL-MoS_2 and ML-MoS_2 in comparison to bulk MoS_2.

The above results demonstrate that MoS_2 nanosheets with controllable layers has been successfully synthesized via a one-step reaction between $(NH_4)_6Mo_7O_{24}$ and CS_2 with appropriately chosen conditions. We propose a possible mechanism for this method. As depicted in Scheme 1, the direct reaction of $(NH_4)_6Mo_7O_{24}$ and CS_2 will form the small 2D domains of MoS_2 and then assemble into multiply-layer MoS_2 nanosheets due to the interaction via Van der Waals force between the layers. When the reaction was assisted with H_2O, the layer-assembling will be partly hindered due to the adsorbed H_2O molecules around them, hence leading to thinner nanosheets. When introducing CNTs in the H_2O-assisted reaction, the CNTs can serve as templates to immobilize the small MoS_2 domains during the reaction, which further hinder the layer-assembling and finally lead to the formation of single layer MoS_2 nanosheets coating on the surface of CNTs. The mechanism of MoS_2 nanosheets growing on CNTs here should be the similar with that on other templates e.g. graphene.[33, 34]

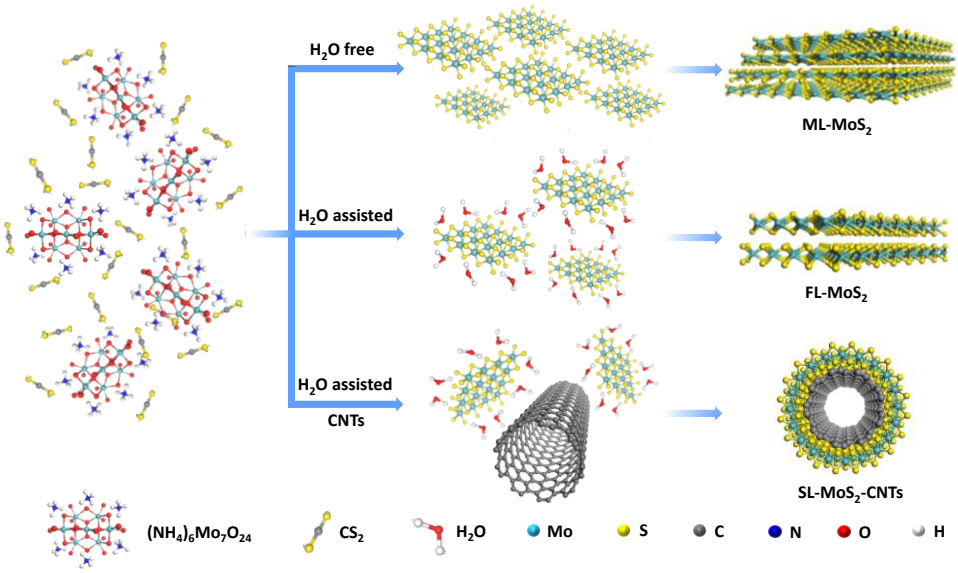

Scheme 1. Schematic illustration for the direct chemical synthesis of multiply-layer MoS_2 (ML-MoS_2), few-layer MoS_2 (FL-MoS_2) and single-layer MoS_2 coating on

carbon nanotubes (SL-MoS_2-CNTs) through modulating the experimental conditions.

2D MoS_2 based nanomaterials have been regard as one promising non-precious catalysts for hydrogen evolution reaction (HER) and stimulated great research interest in the past few years.[35-41] Previous experimental and computational studies indicated that the activity of hydrogen evolution reaction (HER) originates from the edges and defects of MoS_2 nanosheets.[8, 35, 36, 42, 43] It means that increasing the edges and defects in MoS_2 nanosheets will efficiently promote the HER activity. In this study, we find that reducing the layer number of MoS_2 nanosheets will introduce a mass of defects in these nanosheets, as marked in figure 1d and figure S4, implying the HER activity could be enhanced with the layer number of MoS_2 nanosheets reducing. Therefore, we investigate the layer number effect of MoS_2 nanosheets to the HER activity and expect that the optimizing MoS_2 catalysts can enhance the HER performance. The HER electrochemical measurements were performed by using a typical three-electrode setup in 0.1 M H_2SO_4. As shown in Figure 3a, all the prepared MoS_2 samples exhibit high activity compared with bulk MoS_2 and blank glassy carbon (GC) electrode. Moreover, the HER activity increases significantly with layer number of MoS_2 nanosheets reducing, i.e. the HER onset overpotential is ~200 mV for bulk MoS_2, ~110 mV for ML-MoS_2 and ~50 mV for FL-MoS_2, respectively (see table S1). Remarkably, the polarization curve of SL-MoS_2-CNTs shows an onset overpotential of only ~40 mV vs. RHE, beyond which the cathodic current rose rapidly under more negative potentials, and the overpotential at the current density of 10 mA cm^{-2} is 236 mV, showing that SL-MoS_2-CNTs is amongst the most active non-precious HER catalysts in acidic medium.[37, 43-47] In addition, the HER exchange current density (j_0) normalized by the mass loading of these catalysts is also favorably comparable to that of some reported outstanding MoS_2-based catalysts (Table S2). The high HER activity of SL-MoS_2-CNTs may arise from the increase of defects in the single layer, as well as the enhanced electric conductivity by CNTs which promotes the electron transfer during the reaction. Tafel slope is often used to reveal the inherent property of HER electrocatalysts and smaller Tafel slope will lead to faster increment of HER rate with

increasing overpotential.[8] As shown in figure 3b, the Tafel slope of SL-MoS_2-CNTs is 63 mV/dec, much smaller compared with FL-MoS_2 (87 mV/dec) and ML-MoS_2 (110 mV/dec), further confirming that SL-MoS_2-CNTs possesses higher HER activity.

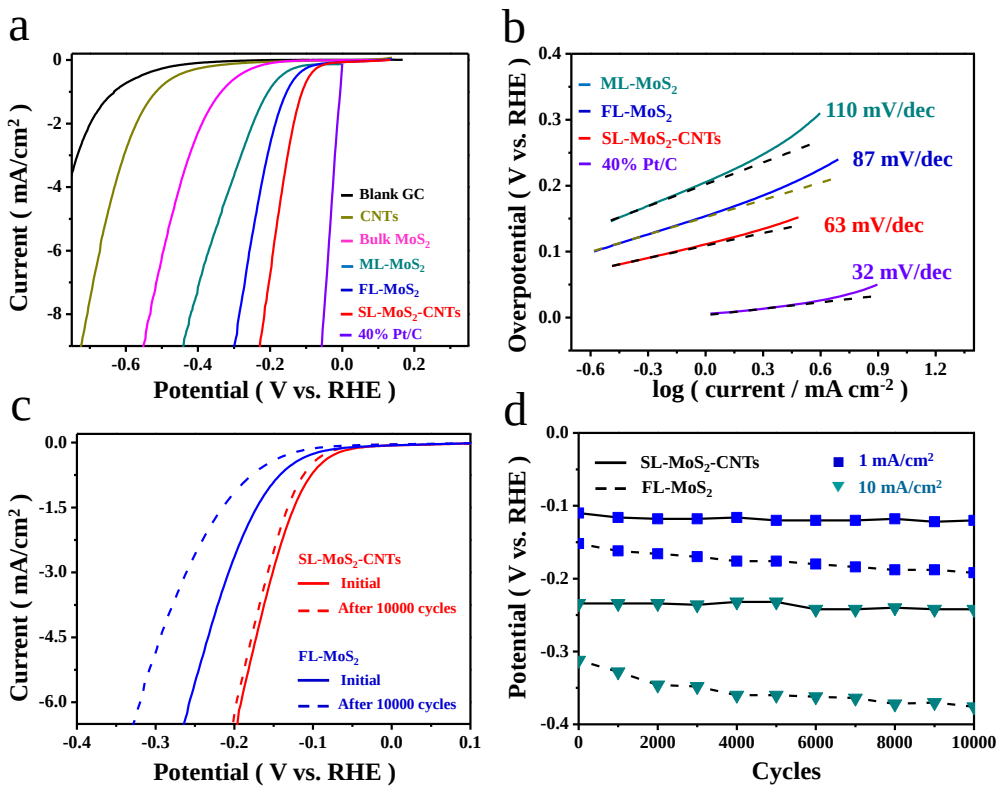

Figure 3. (a) Polarization curves of SL-MoS_2-CNTs, FL-MoS_2, ML-MoS_2 in comparison with bulk MoS_2, CNTs, 40% Pt/C and blank GC electrode. (b) Tafel plots of ML-MoS_2, FL-MoS_2, SL-MoS_2-CNTs and 40% Pt/C. (c) Durability measurements of SL-MoS_2-CNTs and FL-MoS_2. The polarization curves recorded initially and after 10,000 CV sweeps between +0.57 and -0.13 V (vs. RHE). (d) Potential values recorded initially and after every 1000 CV sweeps for SL-MoS_2-CNTs and FL-MoS_2 at 1 mA cm^{-2} and 10 mA cm^{-2}.

Durability is another important criterion to evaluate a HER electrocatalyst. Herein, accelerated degradation experiments were adopted to conduct the evaluation. After every 1000 cyclic voltammetric (CV) sweeps between -0.13 and +0.57 V (vs. RHE), a polarization curve was recorded. From figure 3c, one can see that the SL-MoS_2-CNTs retains almost the same activity as the initial even after 10,000 recycles. In contrast, FL-MoS_2 exhibits an obvious degradation in the activity.

Moreover, from the potential values recorded at the same current density of 1 mA cm^{-2} and 10 mA cm^{-2} with different CV sweeps in figure 3d, one can see that SL-MoS_2-CNTs shows higher durability with negligible overpotential increase compared with FL-MoS_2. Considering more edges and defects will be introduced in MoS_2 nanosheets with the layer number reducing, the structural stability of MoS_2 will reduce and usually lead to the decrease of the catalytic durability. However, in this study, the single-layer MoS_2 on CNTs shows even higher durability than free-standing few-layer nanosheets. We deduce that the introduction of CNTs may enhance the interaction of CNTs and MoS_2 nanosheets, which can efficiently hinder the degradation of the HER durability.

In summary, we introduce a facile and efficient chemical method to directly synthesize 2D MoS_2 nanosheets with controllable layers. Within the method, both free-standing MoS_2 nanosheets and single-layer MoS_2 coating on CNTs can be efficiently prepared via the modulation of experimental conditions. These MoS_2 nanosheets exhibit a significant layer number effect to the hydrogen evolution reaction (HER), i.e. the HER activity will be enhanced with the layer number reducing. Remarkably, the optimized SL-MoS_2-CNTs samples showed long-term durability with more than 10,000 recycles and high HER activity with an onset overpotential of only ~40 mV vs. RHE. These resulting layer-controlled MoS_2 nanosheets are anticipated to find potential application in non-precious HER catalysts as well as in other fields such as electronics and lithium batteries.

Acknowledgements

We gratefully acknowledge the financial support from the National Natural Science Foundation of China (No. 21303191 and 51390474) and the strategic Priority Research Program of the Chinese Academy of Sciences (No. XDA09030100), and thank Prof. Ting Yu at Nanyang Technological University for fruitful discussions on Raman analysis.

References

1. M. S. Xu, T. Liang, M. M. Shi and H. Z. Chen, *Chem. Rev.*, 2013, **113**, 3766-3798.
2. B. Radisavljevic, A. Radenovic, J. Brivio, V. Giacometti and A. Kis, *Nat. Nanotechnol.*, 2011, **6**, 147-150.
3. Q. H. Wang, K. Kalantar-Zadeh, A. Kis, J. N. Coleman and M. S. Strano, *Nat. Nanotechnol.*, 2012, **7**, 699-712.
4. T. Stephenson, Z. Li, B. Olsen and D. Mitlin, *Energy Environ. Sci.*, 2014, **7**, 209-231.
5. M. Chhowalla, H. S. Shin, G. Eda, L. J. Li, K. P. Loh and H. Zhang, *Nature Chem.*, 2013, **5**, 263-275.
6. Z. Wang, T. Chen, W. X. Chen, K. Chang, L. Ma, G. C. Huang, D. Y. Chen and J. Y. Lee, *J. Mater. Chem. A*, 2013, **1**, 2202-2210.
7. M. R. Gao, Y. F. Xu, J. Jiang and S. H. Yu, *Chem. Soc. Rev.*, 2013, **42**, 2986-3017.
8. D. Merki and X. L. Hu, *Energy Environ. Sci.*, 2011, **4**, 3878-3888.
9. J. Yang and H. S. Shin, *J. Mater. Chem. A*, 2014, **2**, 5979-5985.
10. A. B. Laursen, S. Kegnaes, S. Dahl and I. Chorkendorff, *Energy Environ. Sci.*, 2012, **5**, 5577-5591.
11. G. Eda, H. Yamaguchi, D. Voiry, T. Fujita, M. W. Chen and M. Chhowalla, *Nano Lett.*, 2011, **11**, 5111-5116.
12. K. F. Mak, C. Lee, J. Hone, J. Shan and T. F. Heinz, *Phys. Rev. Lett.*, 2010, **105**, 136805-136808.
13. Y. J. Zhang, J. T. Ye, Y. Matsuhashi and Y. Iwasa, *Nano Lett.*, 2012, **12**, 1136-1140.
14. K. S. Novoselov, D. Jiang, F. Schedin, T. J. Booth, V. V. Khotkevich, S. V. Morozov and A. K. Geim, *Proc. Natl. Acad. Sci.*, 2005, **102**, 10451-10453.
15. H. Li, Z. Y. Yin, Q. Y. He, H. Li, X. Huang, G. Lu, D. W. H. Fam, A. I. Y. Tok, Q. Zhang and H. Zhang, *Small*, 2012, **8**, 63-67.
16. J. N. Coleman, M. Lotya, A. O'Neill, S. D. Bergin, P. J. King, U. Khan, K. Young, A. Gaucher, S. De, R. J. Smith, I. V. Shvets, S. K. Arora, G. Stanton, H. Y. Kim, K. Lee, G. T. Kim, G. S. Duesberg, T. Hallam, J. J. Boland, J. J. Wang, J. F. Donegan, J. C. Grunlan, G. Moriarty, A. Shmeliov, R. J. Nicholls, J. M. Perkins, E. M. Grieveson, K. Theuwissen, D. W. McComb, P. D. Nellist and V. Nicolosi, *Science*, 2011, **331**, 568-571.
17. K. G. Zhou, N. N. Mao, H. X. Wang, Y. Peng and H. L. Zhang, *Angew. Chem. Int. Ed.*, 2011, **50**, 10839-10842.
18. H. S. S. R. Matte, A. Gomathi, A. K. Manna, D. J. Late, R. Datta, S. K. Pati and C. N. R. Rao, *Angew. Chem. Int. Ed.*, 2010, **49**, 4059-4062.
19. Z. Y. Zeng, Z. Y. Yin, X. Huang, H. Li, Q. Y. He, G. Lu, F. Boey and H. Zhang, *Angew. Chem. Int. Ed.*, 2011, **50**, 11093-11097.
20. A. Castellanos-Gomez, M. Barkelid, A. M. Goossens, V. E. Calado, H. S. J. van der Zant and G. A. Steele, *Nano Lett.*, 2012, **12**, 3187-3192.
21. Y. G. Yao, Z. Y. Lin, Z. Li, X. J. Song, K. S. Moon and C. P. Wong, *J. Mater. Chem.*, 2012, **22**, 13494-13499.
22. X. S. Wang, H. B. Feng, Y. M. Wu and L. Y. Jiao, *J. Am. Chem. Soc.*, 2013, **135**, 5304-5307.
23. W. J. Zhang, J. K. Huang, C. H. Chen, Y. H. Chang, Y. J. Cheng and L. J. Li, *Adv. Mater.*, 2013, **25**, 3456-3461.
24. C. Altavilla, M. Sarno and P. Ciambelli, *Chem. Mater.*, 2011, **23**, 3879-3885.
25. Y. Y. Peng, Z. Y. Meng, C. Zhong, J. Lu, W. C. Yu, Y. B. Jia and Y. T. Qian, *Chem. Lett.*, 2001, **30**, 772-773.

26. M. M. Mdleleni, T. Hyeon and K. S. Suslick, *J. Am. Chem. Soc.*, 1998, **120**, 6189-6190.
27. R. Tenne, *Nat. Nanotechnol.*, 2006, **1**, 103-111.
28. H. Li, Q. Zhang, C. C. R. Yap, B. K. Tay, T. H. T. Edwin, A. Olivier and D. Baillargeat, *Adv. Funct. Mater.*, 2012, **22**, 1385-1390.
29. C. Lee, H. Yan, L. E. Brus, T. F. Heinz, J. Hone and S. Ryu, *ACS Nano*, 2010, **4**, 2695-2700.
30. G. Plechinger, S. Heydrich, J. Eroms, D. Weiss, C. Schuller and T. Korn, *Appl. Phys. Lett.*, 2012, **101**, 101906.
31. M. Virsek, A. Jesih, I. Milosevic, M. Damnjanovic and M. Remskar, *Surf. Sci.*, 2007, **601**, 2868-2872.
32. E. Scalise, M. Houssa, G. Pourtois, V. V. Afanasev and A. Stesmans, *Physica. E*, 2014, **56**, 416-421.
33. K. Chang and W. X. Chen, *Chem. Commun.*, 2011, **47**, 4252-4254.
34. X. S. Zhou, L. J. Wan and Y. G. Guo, *Chem. Commun.*, 2013, **49**, 1838-1840.
35. B. Hinnemann, P. G. Moses, J. Bonde, K. P. Jorgensen, J. H. Nielsen, S. Horch, I. Chorkendorff and J. K. Nørskov, *J. Am. Chem. Soc.*, 2005, **127**, 5308-5309.
36. T. F. Jaramillo, K. P. Jorgensen, J. Bonde, J. H. Nielsen, S. Horch and I. Chorkendorff, *Science*, 2007, **317**, 100-102.
37. Y. G. Li, H. L. Wang, L. M. Xie, Y. Y. Liang, G. S. Hong and H. J. Dai, *J. Am. Chem. Soc.*, 2011, **133**, 7296-7299.
38. J. F. Xie, H. Zhang, S. Li, R. X. Wang, X. Sun, M. Zhou, J. F. Zhou, X. W. Lou and Y. Xie, *Adv. Mater.*, 2013, **25**, 5807.
39. H. T. Wang, Z. Y. Lu, S. C. Xu, D. S. Kong, J. J. Cha, G. Y. Zheng, P. C. Hsu, K. Yan, D. Bradshaw, F. B. Prinz and Y. Cui, *Proc. Natl. Acad. Sci.*, 2013, **110**, 19701-19706.
40. T. Y. Wang, L. Liu, Z. W. Zhu, P. Papakonstantinou, J. B. Hu, H. Y. Liu and M. X. Li, *Energy Environ. Sci.*, 2013, **6**, 625-633.
41. Y. F. Yu, S. Y. Huang, Y. P. Li, S. N. Steinmann, W. T. Yang and L. Y. Cao, *Nano Lett.*, 2014, **14**, 553-558.
42. H. I. Karunadasa, E. Montalvo, Y. J. Sun, M. Majda, J. R. Long and C. J. Chang, *Science*, 2012, **335**, 698-702.
43. J. Kibsgaard, Z. B. Chen, B. N. Reinecke and T. F. Jaramillo, *Nat. Mater.*, 2012, **11**, 963-969.
44. J. F. Xie, J. J. Zhang, S. Li, F. Grote, X. D. Zhang, H. Zhang, R. X. Wang, Y. Lei, B. C. Pan and Y. Xie, *J. Am. Chem. Soc.*, 2013, **135**, 17881-17888.
45. J. Deng, P. J. Ren, D. H. Deng, L. Yu, F. Yang and X. H. Bao, *Energy Environ. Sci.*, 2014, **7**, 1919-1923.
46. Z. B. Chen, D. Cummins, B. N. Reinecke, E. Clark, M. K. Sunkara and T. F. Jaramillo, *Nano Lett.*, 2011, **11**, 4168-4175.
47. T. F. Jaramillo, J. Bonde, J. D. Zhang, B. L. Ooi, K. Andersson, J. Ulstrup and I. Chorkendorff, *J. Phys. Chem. C*, 2008, **112**, 17492-17498.